CHEMISTRY OF MATERIALS
Article

Chem. Mater. **2010,** *22,* 2255–2260 2255
DOI:10.1021/cm9030733

Tunable, Ligand-Based Emission from Inorganic−Organic Frameworks: A New Approach to Phosphors for Solid State Lighting and Other Applications

Joshua D. Furman,[†,‡] Alina Y. Warner,[‡] Simon J. Teat,[§] Alexander A. Mikhailovsky,[⊥] and Anthony K. Cheetham*,[†]

[†]*Department of Materials Science and Metallurgy, University of Cambridge, United Kingdom CB2 3QZ,* [‡]*Mitsubishi Chemical Center for Advanced Materials, University of California, Santa Barbara, California 93106,* [§]*Advanced Light Source, Lawrence Berkeley National Laboratory, 1 Cyclotron Road, Mail Stop 2-400, Berkeley, California 94720, and* [⊥]*ChemistryDepartment, University of California, Santa Barbara, California 93106*

Received October 3, 2009. Revised Manuscript Received January 27, 2010

Two dense inorganic−organic frameworks were prepared using the intrinsically luminescent organic ligand 9-fluorenone-2,7-dicarboxylic acid (H_2FDC) in combination with the alkaline earth metals calcium and strontium. $Ca(FDC)(H_2O)_2$ (**1**) and $Sr(FDC)(H_2O)_5 \cdot 2H_2O$ (**2**) were prepared hydrothermally and both adopt three-dimensional framework structures. They absorb strongly between 380 and 460 nm and show broad visible emission with peaks at 503 and 526 nm, respectively. Structure **1** shows a quantum yield at room temperature of 7.8% which increases to 15% at −196 °C, while structure **2** shows a room temperature quantum yield of 2.8%, increasing to 3.3% at −196 °C.

Introduction

Solid state lighting in the form of white light-emitting diodes (LEDs) is poised to replace incandescent and mercury-containing fluorescent lighting in the near future.[1,2] Today's commercial devices use InGaN in combination with a yellow phosphor, typically Ce^{3+}-doped yttrium aluminum garnet.[3−5] This combination of blue and yellow is inexpensive and efficient but has poor color-rendering properties. Consequently, there has been an extensive search in the past decade for new phosphor materials that have broad emissions in the green, yellow, and red spectra.[6] Ideally, a solid state lighting phosphor will have be excited in the blue or near-UV and emit broadly in the green-to-red regions to create a broad spectrum white light similar to blackbody radiation.[7] Thermal stability of the emitted light color and intensity is also critical as the temperature inside an LED device can reach over 100 °C.[8] The vast majority of newly reported compounds are rare-earth doped oxides[9−13] and nitrides.[14,15] Alternatively, while much work has been carried out on electroluminescent materials (OLEDs) for displays, organic photoluminescent materials are unlikely to meet the stability requirements for lighting applications. We present here an intermediate approach to phosphors for solid state lighting, using inorganic−organic (hybrid) framework structures that are more commonly associated with applications like gas storage and catalysis. Hybrid frameworks are typically more stable than organic materials and have certain advantages over inorganics.

The field of hybrid framework research has grown rapidly in the past two decades due to the discovery of materials that exhibit a wide range of structural diversity[16] and physical phenomena.[17,18] A recent review profiled hybrid structures for luminescence, listing potential applications as sensors, scintillators, and nonlinear optical materials.[19] Solid state

*To whom correspondence should be addressed. E-mail: akc30@cam.ac.uk.

(1) Nakamura, S.; Fasol, G. *The blue laser diode: GaN based blue light emitters*; Springer: Berlin, 1997.
(2) Shur, M. S.; Žukauskas, A. *Proc. IEEE* **2005**, *93*, 1691.
(3) Blasse, G.; Bril, A. *J. Chem. Phys.* **1967**, *47*, 5139–5145.
(4) Blasse, G.; Bril, A. *Appl. Phys. Lett.* **1967**, *11*, 53–54.
(5) Schlotter, P.; Schmidt, R.; Schneider, J. *Appl. Phys. A: Mater. Sci. Process.* **1997**, *64*, 417.
(6) Zachau, M.; Becker, D.; Berben, D.; Fiedler, T.; Jermann, F.; Zwaschka, F. *Proc. SPIE* **2008**, *6910*, 691010.
(7) Energy Efficient Lighting and Light Emitting Diodes. http://www.netl.doe.gov/ssl/usingLeds/ (accessed **2006**).
(8) Meneghini, M.; Trevisanello, L.-R.; de Zuani, F.; Trivellin, N.; Meneghesso, G.; Zanoni, E. Extensive analysis of the degradation of phosphor-converted LEDs. *SPIE Ninth International Conference on Solid State Lighting*, San Diego, CA, 3 August 2009; Vol. *7422*, p 74220H.
(9) Neeraj, S.; Kijima, N.; Cheetham, A. K. *Chem. Phys. Lett.* **2004**, *387*, 2–6.
(10) Sohn, K. S.; Park, D. H.; Cho, S. H.; Kwak, J. S.; Kim, J. S. *Chem. Mater.* **2006**, *18*, 1768–1722.
(11) Yoo, H. S.; Im, W. B.; Kang, J. H.; Jeon, D. Y. *Opt. Mater.* **2008**, *31*, 131–135.
(12) Im, W. B.; Fellows, N. N.; DenBaars, S. P.; Seshadri, R.; Kim, Y. I. *Chem. Mater.* **2009**, *21*, 2957–2966.
(13) Neeraj, S.; Kijima, N.; Cheetham, A. K. *Solid State Commun.* **2004**, *131*, 65–69.
(14) Mueller-Mach, R.; Mueller, G.; Krames, M. R.; Höppe, H. A.; Stadler, F.; Schnick, W.; Juestel, T.; Schmidt, P. *Phys. Status Solidi A* **2005**, *202*, 1727–1723.
(15) Toquin, R. L.; Cheetham, A. K. *Chem. Phys. Lett.* **2006**, *423*, 352–356.
(16) Cheetham, A. K.; Rao, C. N. R.; Feller, R. K. *Chem. Commun.* **2006**, *46*, 4780–4795.
(17) Kitagawa, S.; Kitaura, R.; Noro, S. *Angew. Chem., Int. Ed.* **2004**, *43*, 2334–2375.
(18) Rao, C. N. R.; Cheetham, A. K.; Thirumurugan, A. *J. Phys.: Condens. Matter* **2008**, *20*, 159801.
(19) Allendorf, M. D.; Bauer, C. A.; Bhakta, R. K.; Houk, R. J. T. *Chem. Soc. Rev.* **2009**, *38*, 1330–1352.

Published on Web 02/17/2010

lighting was not considered as a potential application, probably because very few luminescent inorganic−organic papers give details of the excitation and quantum yield data that is critical for lighting efficiency.

Luminescence from hybrid structures can exist in several forms. The most common involves an antenna-like process in which the organic ligand absorbs incident energy and there is charge transfer to a luminescent metal species. Photoluminescence can also arise from direct metal excitation in which the organic ligands act as spacers to reduce cross-relaxation and quenching. Both of these approaches are typically seen with rare-earth ions and have long been utilized in coordination compounds.[20] Rare-earth-based luminescence from well-defined f → f transitions in Eu^{3+} and Tb^{3+} give sharp emission peaks. This type of photoluminescence is useful for display applications and is found in some fluorescent tube devices; however, to achieve true blackbody quality color rendering, phosphors with broad emission spectra and, ideally, color tunability are required.[21,22] Ce^{3+}- and Eu^{2+}-containing inorganic phosphors are commonly used for lighting as they provide broad emission bands from d → f transitions, their emission color can be tuned by ligand field effects,[23,24] and the excitation of their dipole-allowed transitions aligns with the emission wavelengths of InGaN LEDs.

Ligand-based emission, where closed-shell metal ions act to stabilize an intrinsically luminescent organic, is less common. A few hybrid structures showing this type of ligand-centered luminescence have been described,[25−33] but all of them report excitation wavelengths in the UV and emission wavelengths that peak around 420 nm. Since a large portion of the emission lies out of the visible range, such materials are clearly not suitable for solid state lighting applications. However, in the case of the zinc−stilbene system, the excitation and emission were tunable in the UV and blue, respectively.[34]

Here, we present the photoluminescent properties of 9-fluorenone-2,7-dicarboxylate in combination with calcium and strontium. These inorganic−organic framework materials exhibit broad, ligand-based emission that can be tuned by changing the cation. The quantum yields are enhanced relative to the ligand alone due to the conformation rigidity of the hybrid structure. These new materials possess many of the properties required for a phosphor for solid state lighting.

Experimental Methods

Synthesis. 9-Fluorenone-2,7-dicarboxylic acid (H_2FDC) was obtained from Trans World Chemicals and used without further purification. All other reagents were obtained from Sigma-Aldrich. Hydrothermal reactions were carried out in 23 mL PTFE lined Parr brand autoclaves using deionized water.

Preparation of Na_2FDC. The sodium salt of FDC (Na_2FDC) was prepared by combining equimolar amounts of NaOH and H_2FDC in water. The solution was stirred overnight and evaporated to dryness on a hot plate. The crude product was refluxed in ethanol for 1 h, separated by filtration, and dried under vacuum at room temperature. The sodium salt shows high water solubility at room temperature whereas the acid was only sparingly soluble in water.

Preparation of CaFDC. $Ca(FDC)(H_2O)_2$ (**1**) was prepared from 0.05 mmol of calcium acetate, 0.05 mmol Na_2FDC, and 5 mL H_2O. The mixture was stirred, sealed in an autoclave, and heated to 150 °C for 2 days before cooling to room temperature. Tiny yellow needle crystals were recovered by filtration and washed with water and acetone. Phase pure powders in greater yield were prepared by reacting equimolar amounts of calcium acetate and H_2FDC in water hydrothermally at 150 °C. CHN analysis performed by the Marine Sciences Institute Analytical Laboratory at UCSB found 52.65% C, 2.91% H; calculated 52.63% C, 2.94% H.

Preparation of SrFDC. $Sr(FDC)(H_2O)_5 \cdot 2H_2O$ (**2**) was prepared from 0.05 mmol strontium acetate, 0.05 mmol H_2FDC, 0.05 mmol imidazole, and 5 mL H_2O. The mixture was stirred, sealed in an autoclave, and heated to 180 °C for 2 days before cooling to room temperature. Small yellow plate crystals were recovered by filtration. Although imidazole was not incorporated into the structure, its presence was required to obtain single crystal products. Phase pure powders were prepared by reacting equimolar amounts of strontium acetate and H_2FDC hydrothermally at 180 °C. CHN analysis found 40.75% C, 3.12% H; calculated: 37.54% C, 4.20% H.

Structure Determination. All structures were determined using single crystal X-ray diffraction. Data collection for **1** was performed on beamline 11.3.1 at the Advanced Light Source at Lawrence Berkeley National Laboratory (λ = 0.77490 Å). A crystal was mounted on a Kaptan loop using paratone-N oil and placed in a LN_2 cryostream at 100 K. Data were collected using a Bruker goniometer and APEX II detector. Data integration and corrections for Lorentz and polarization effects were performed using Bruker SAINT version 7.56a.[35] SADABS was used

(20) Sabbatini, N.; Guardigli, M. *Coord. Chem. Rev*. **1993**, *123*, 201–228.
(21) Fukui, T.; Kamon, K.; Takeshita, J.; Hayashi, H.; Miyachi, T.; Uchida, Y.; Kurai, S.; Taguchi, T. *Jpn. J. Appl. Phys*. **2009**, *48*, 112101.
(22) Mirhosseini, R.; Schubert, M.; Chhajed, S.; Cho, J.; Kim, J. K.; Schubert, E. F. Color rendering ability and luminous efficacy enhancements in white light-emitting diodes. *Proceedings of the SPIE Ninth International Conference on Solid State Lighting*, San Diego, CA, 3 August 2009; p 742212.
(23) Wu, J. L.; Gundiah, G.; Cheetham, A. K. *Chem. Phys. Lett*. **2007**, *441*, 250–254.
(24) Bachmann, V.; Ronda, C.; Oeckler, O.; Schnick, W.; Meijerink, A. *Chem. Mater*. **2009**, *21*, 316–325.
(25) Du, M.; Jiang, X. J.; Zhao, X. J. *Inorg. Chem*. **2007**, *46*, 3984–3995.
(26) Wang, X.-L.; Bi, Y.-F.; Lin, H.-Y.; Liu, G.-C. *Cryst. Growth Des*. **2007**, *7*, 1086–1091.
(27) Chen, Z.-F.; Xiong, R.-G.; Zhang, J.; Chen, X.-T.; Xue, Z.-L.; You, X.-Z. *Inorg. Chem*. **2001**, *40*, 4075–4077.
(28) Lu, Z.; Wen, L.; Ni, Z.; Li, Y.; Zhu, H.; Meng, Q. *Cryst. Growth Des*. **2007**, *7*, 268–274.
(29) Lin, J.-G.; Xu, Y.-Y.; Qiu, L.; Zang, S.-Q.; Lu, C.-S.; Duan, C.-Y.; Li, Y.-Z.; Gao, S.; Meng, Q.-J. *Chem. Commun*. **2008**, 2659–2661.
(30) Li, M.-X.; Miao, Z.-X.; Shao, M.; Liang, S.-W.; Zhu, S.-R. *Inorg. Chem*. **2008**, *47*, 4481–4489.
(31) Song, L.; Du, S. W.; Lin, J. D.; Zhou, H.; Li, T. *Cryst. Growt Des*. **2007**, *7*, 2268–2271.
(32) Ouyang, X. M.; Li, Z. W.; Okamura, T. A.; Li, Y. Z.; Sun, W. Y.; Tang, W. X.; Ueyama, N. *J. Solid State Chem*. **2004**, *177*, 350–360.
(33) Wu, W. P.; Wang, Y. Y.; Wang, C. J.; Wu, Y. P.; Liu, P.; Shi, Q. Z. *Inorg. Chem. Commun*. **2006**, *9*, 645–648.
(34) Bauer, C. A.; Timofeeva, T. V.; Settersten, T. B.; Patterson, B. D.; Liu, V. H.; Simmons, B. A.; Allendorf, M. D. *J. Am. Chem. Soc*. **2007**, *129*, 7316–7144.
(35) *SAINT Frame Integration Software*; Bruker AXS Inc.: Madison, WI, 2000.

Table 1. Crystal Data for 1 and 2

	1	2
formula	$CaC_{15}O_7H_{10}$	$Sr_2C_{30}O_{17}H_{26}$
MW (g/mol)	342.31	833.75
system	monoclinic	triclinic
space group	$P2_1$	$P\bar{1}$
a (Å)	7.5411(16)	8.578(2)
b (Å)	6.6118(14)	11.836(3)
c (Å)	27.999(6)	15.626(4)
α (deg)	90	72.437(4)
β (deg)	97.065(3)	78.722(5)
γ (deg)	90	85.437(4)
V (Å^3)	1385.4(5)	1483.1(7)
Z	4	2
ρ (g/cm^3)	1.641	1.867
μ (mm^{-1})	0.613	3.683
measurement temp (K)	100	298
radiation source	synchrotron	Mo Kα
radiation λ (Å)	0.7749	0.71073
scan mode	omega	omega
absorption correction	SADABS	SADABS
solution method	SHELX, $\|F\|^2$	SHELX, $\|F\|^2$
2θ range (deg)	2.97−29.36	4.834−51.953
data/restraints/parameters	5824/440/130	5902/487/21
R_1/wR_2 [$I > 2\sigma(I)$]	8.19%/21.84%	5.71%/18.06%
R_1/wR_2 (all data)	8.56%/22.22%	10.13%/13.00%
goodness of fit	1.046	1.029

to perform an absorption correction.[36] The high brightness synchrotron source allowed for the analysis of very small crystals. Data were collected for **2** on a Siemens SMART-CCD diffractometer at UCSB equipped with a normal focus, 2.4 kW sealed tube X-ray source (Mo Kα radiation, λ = 0.71073 Å) operating at 45 kV and 30 mA and integrated with Bruker Saint version 6.02.[35] Suitable single crystals were selected under a polarizing microscope and glued to a glass fiber, and a hemisphere of intensity data was collected at room temperature. SADABS was used to perform an absorption correct and both structures were then solved by direct methods and difference Fourier synthesis and were refined against $|F|^2$ using the SHELXL software package.[36,37] Details of the structure determination are shown in Table 1. All extinction coefficients refined to within three esd's of zero and were therefore removed from the refinement. Non-hydrogen atoms were refined anisotropically. Riding hydrogens were assigned to the carbon atoms on the FDC ligands. Hydrogen atoms on the water molecules were found in the Fourier difference map and were refined isotropically. Hydrogen atoms were restrained to chemically appropriate positions, resulting in increased residual error.

Powder diffraction data were collected at the Advanced Photon Source synchrotron X-ray beamline 11-BM at λ = 0.589183 Å for **1** and on a Bruker D8 with Cu Kα source for **2**. Models were refined to the data using GSAS and EXPGUI[38,39] to confirm purity of the bulk sample (see the Supporting Information).

Room temperature photoluminescence spectra were collected on a Perkin-Elmer LS55 spectrometer using finely ground powders mounted behind a quartz window. Quantum yield data were collected on solid samples mounted on quartz slides in silicone resin. The samples were placed within an integrating sphere and excited with a 405 nm laser. Temperature-dependent emission spectra were collected using the same 405 nm excitation and a LN_2 cooled cryostat in combination with an Acton Research spectrometer.

(36) Sheldrick, G. M. *SADABS User Guide*; University of Göttingen: Göttingen, Germany, 1995.
(37) Sheldrick, G. *Acta Crystallogr.* **2008**, *A64*, 112–122.
(38) Larson, A. C.; Von Dreele, R. B. Los Alamos National Laboratory Report LAUR; **2000**; pp 86−748.
(39) Toby, B. H. *J. Appl. Crystallogr.* **2001**, *34*, 210–213.

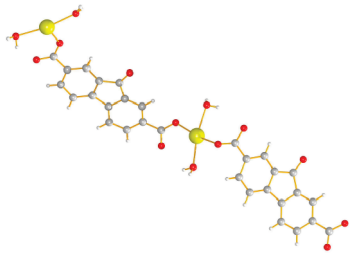

Figure 1. Asymmeteric unit of **1**.

Results and Discussion

Structures. The structure of $Ca(FDC)(H_2O)_2$ (**1**; Figure 1) consists of isolated CaO_6 octahedra linked through FDC ligands as seen in Figure 2a. Each octahedron connects to four FDC ligand oxygen atoms and two coordinating water molecules, while each dicarboxylic acid oxygen atom of the FDC ligand is bound to a different metal. The octahedra arrange in sheets which are pillared by FDC ligands to form a three-dimensional structure (Figure 2b) without porosity. The ligands are π-stacked with the ketone groups aligned. Obtaining high quality crystals of **1** was very difficult, but with the use of synchrotron radiation we were able to obtain a satisfactory structure that was consistent with the powder X-ray diffraction and thermal gravimetric analysis results.

The structure of $Sr(FDC)(H_2O)_5\cdot 2H_2O$ (**2**; Figure 3) consists of edge-sharing SrO_8 polyhedra that form one-dimensional chains (Figure 4a). These chains are linked in-plane by the carboxylic acid groups of the FDC ligand to form a sheet, and the sheets are in turn bridged by the FDC to form an extended three-dimensional framework without porosity, seen in Figure 4b. The strontium atoms in the chains are arranged in pairs of two Sr1 atoms followed by two Sr2 atoms, with atom−atom distances of Sr1−Sr1 4.5674 Å, Sr1−Sr2 3.9935 Å, and Sr2−Sr2 4.0966 Å. The Sr1 polyhedra is completed by two coordinating water molecules, three bridging water molecules, and three oxygen atoms from carboxylic acid groups on the ligand. The Sr2 polyhedra consists of one coordinating water, one bridging water, and six oxygen atoms from the ligand. Two zeolitic water molecules sit in the pore space. One of the four dicarboxylic acid group oxygens on each FDC ligand is uncoordinated. The ligands π-stack less perfectly than those of structure **1**, with the ketone groups alternating in direction. Bonding arrangements of the ligand with respect to the adjacent metals are shown in Figure 5, where it can be seen that there is more structural rigidity for the calcium containing framework as all of its dicarboxylate oxygens are bound to metal cations.

Luminescence. Room temperature excitation and emission curves of H_2FDC, **1**, and **2** show broad emission that is yellow for the ligand itself, blue-shifted into the green for the calcium structure, and red-shifted into the orange for the strontium structure (Figure 6). The excitation curve of H_2FDC (Figure 6), measured at λ_{em} = 500 nm, shows strong peaks near 390 and 440 nm and then decreases sharply. The accompanying emission curve, measured at λ_{em} = 440 nm, shows a broad emission

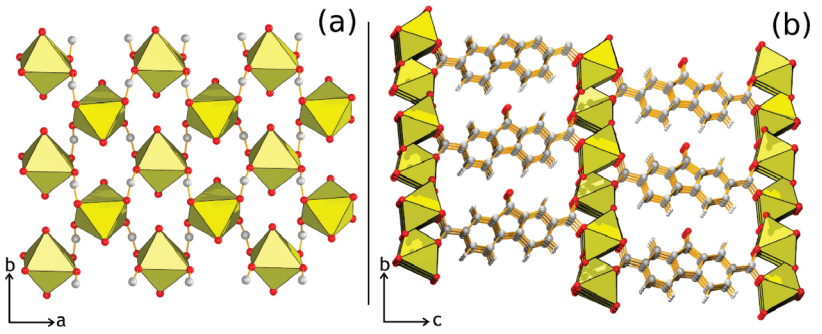

Figure 2. (a) Sheet of isolated CaO octahedra of **1** with hydrogen atoms omitted for clarity viewed down the *c* axix. (b) Extended structure viewed down the *c* axis.

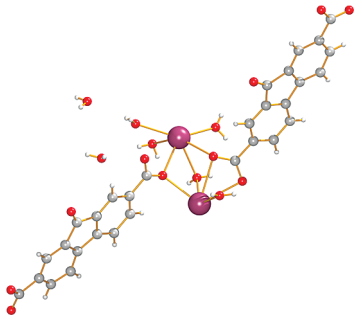

Figure 3. Asymmeteric unit of **2**.

centered at 515 nm. The excitation curve of **1** (Figure 6), measured under the same conditions, is mostly constant into the blue and drops sharply at 460 nm. The emission curve, measured at λ_{em} = 440 nm, peaks at 503 nm with a long tail into the red. Similarly, the excitation of **2** (Figure 6) drops sharply at 460 nm and the emission peaks at 526 nm. Prior work has shown the emission quantum yield and color of the nonfunctionalized molecule 9-fluorenone to be solvent dependent.[40] Kobayashi and Nagakura found shifts in both the singlet and triplet state positions of 9-fluorenone depending on the polarity of the solvent.[41] Changing the band structure of the extended network by altering cation choice and atomic arrangements could well be creating a solvent-like effect which would account for the change in emission color. Alternatively, differences in interligand interactions could account for the shift.

The room temperature quantum yield (QY) of **1** was measured at 7.4%, **2** at 2.8%, and the ligand H_2FDC at 2.4%. The value for the ligand is similar to the range reported for 9-fluorenone in acetonitrile at 2.7−3.4%[40,42,43] Additionally, we see significantly more overlap of the excitation and emission spectra in Figure 6 for **2** and H_2FDC than in **1**. This spectral overlap could indicate increased reabsorption and be a cause of the lower QY for **2**. Concentration quenching could not be directly evaluated as any substitution of the chromophor with an optically nonactive ligand would alter the structure and thus distort the results. However, we expect decreased concentration quenching as compared to a dense oxide phosphor system do to the increased isolation of the ligands by their inclusion in the framework structure. Nevertheless, the ligand to ligand separation of 3.5 Å is still short enough that we expect some energy migration between the emission centers, although in the crystal structure there is no bonding along this distance. In light of the high concentration of emitters, the 7.4% quantum yield in **1** is remarkable.

Temperature dependent emission spectra show an increase in emission intensity with no color shifting on cooling from room temperature to −196 °C for both H_2FDC and **1** (Figure 7). The temperature dependent emission intensity of **2** was largely constant on cooling and decreased at temperatures above 100 °C. The extrapolated temperature dependent QY data is shown in Figure 8. At −196 °C, the QY is of **1** is 15%, approximately double its value at room temperature. This decrease in quantum yield is an effect of thermally generated phonon modes providing nonradiative decay pathways for excitons. Theory would predict an inverse-S type curve where at low temperatures the phonon modes are frozen and at high temperatures the phonon modes are saturated, with a transition range at intermediate temperatures.[44] The curves for H_2FDC and **1** suggest that the measured temperature range falls within the intermediate transition range. The relative stability but lower absolute values in the QY of **2** suggest that it lies within the fully saturated region and further cooling would produce an increase in intensity. If **2** is in the fully saturated region of the curve, then in addition to thermal quenching there must also be some amount of concentration quenching; otherwise, theory would predict a lower nonradiative recombination rate and thus higher quantum yield.[44] Further, the increased spectral overlap from broadened bands at increased temperatures leads to an increase in spectral overlap and thus a temperature dependent increase in concentration quenching.

The stability of the temperature dependent emission properties is important as the junction temperature of blue LEDs can reach over 100 °C, particularly in the new high power, high brightness device designs. A reduced emission

(40) Andrews, L. J.; Deroulede, A.; Linschitz, H. *J. Phys. Chem.* **1978**, *82*, 2304–2309.
(41) Kobayashi, T.; Nagakura, S. *Chem. Phys. Lett.* **1976**, *43*, 429–434.
(42) Murphy, R. S.; Moorlag, C. P.; Green, W. H.; Bohne, C. *J. Photochem. Photobiol. A: Chem.* **1997**, *110*, 123–129.
(43) Singer, L. A. *Tetrahedron Lett.* **1969**, *12*, 923–926.
(44) Yen, W. M.; Shionoya, S.; Yamamoto, H. *Phosphor Handbook*; CRC Press: Boca Raton, 1998; pp 35−47.

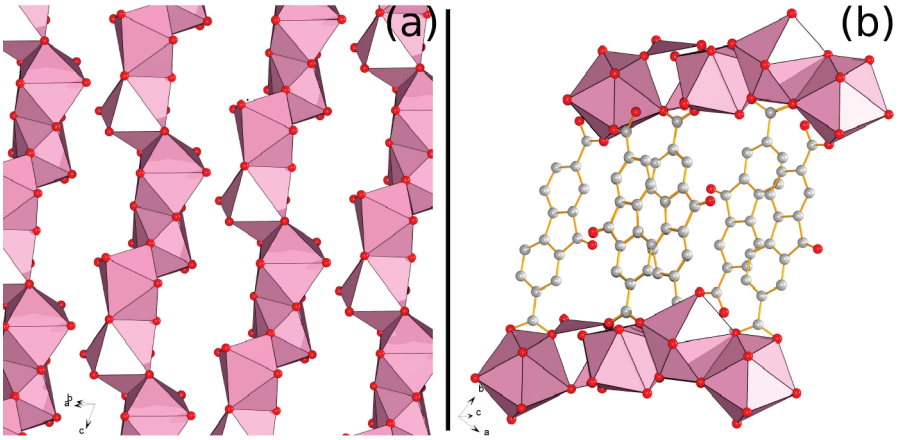

Figure 4. (a) One-dimensional edge sharing SrO_8 chains in **2**. (b) Extended structure.

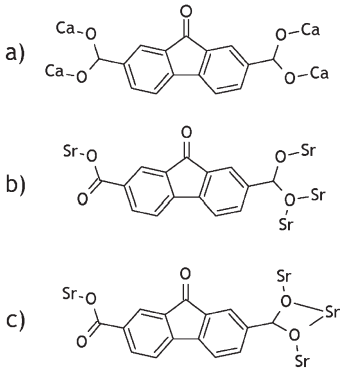

Figure 5. (a) Bonding arrangement of **1**. (b and c) Bonding arrangement of **2**.

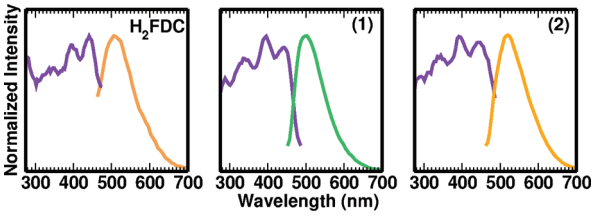

Figure 6. Emission and excitation spectra of H_2FDC, **1**, and **2** (as labeled) at λ_{ex} = 440 nm, λ_{em} = 500 nm.

intensity with temperature would lead to a blue-shift and intensity decrease in the output light. Vibrational studies and wider temperature ranges were not within the scope of this research but would further elucidate the behavior of this system.

We propose that the increased brightness of **1** with respect to H_2FDC may be a result of the covalent bonding to a metal network providing far more structural rigidity than the hydrogen bonding of an organic crystal or even the more flexible arrangements of a cross-linked polymer. That the quantum yield of **1** is roughly 3 times that of **2** may be explained by the rigidity provided by the increased carboxylate-oxygen bonding seen in Figure 5, where each dicarboxylate oxygen is bound to a Ca in (**1**) while one of every four dicarboxylate oxygen atoms in **2** is unbound. The increased ligand π-stacking in **1** may also be strengthening the rigidity and enhancing luminescence.

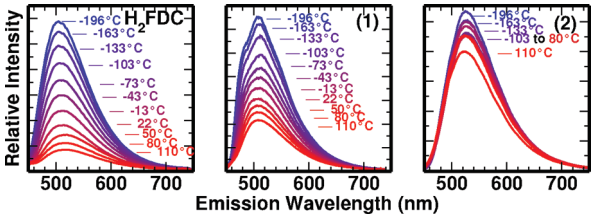

Figure 7. Temperature dependent emission spectra (λ_{ex} = 405 nm) of H_2FDC, **1**, and **2** (as labeled).

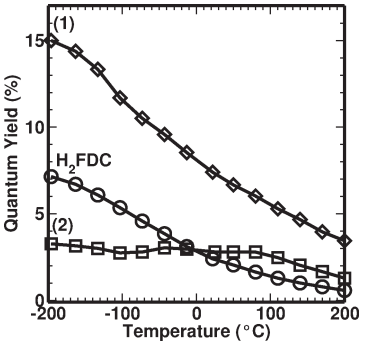

Figure 8. Temperature dependent QY of H_2FDC, **1**, and **2**.

It has been reported that increased π-stacking leads to a reduction in quantum yield for conjugated polymers because of increased aggregate formation and thus increased nonradiative cross-relaxation between ligands.[45−47] The theoretical analysis of Cornil et al. considered cofacial dimers of stilbene molecules and found that the molecular orbitals of the dimer pair begin to delocalize with a chain spacing below 5 Å.[48] The FDC units in **1** are separated by 3.5 Å with an interplane angle of 2°. However, we see an enhancement of the quantum yield in **1** over both H_2FDC and **2** where the ligand units are more staggered. We consider it unlikely that orbital degeneracy between the ligand units is as important in **1** as it is in the conjugated

(45) Amrutha, S. R.; Jayakannan, M. *J. Phys. Chem. B* **2006**, *110*, 4083–4091.
(46) Amrutha, S. R.; Jayakannan, M. *J. Phys. Chem. B* **2008**, *112*, 1119–1129.
(47) Akcelrud, L. *Prog. Poym. Sci* **2003**, *28*, 875–962.
(48) Cornil, J.; dos Santos, D. A.; Crispin, X.; Silbey, R.; Brédas, J. L. *J. Am. Chem. Soc.* **1998**, *120*, 1289–1299.

polymer chains or theoretical dimer systems. Moreover, it is the cyclic dimerization possible in a more flexible polymer chain that reduces quantum yield, a process not expected in a rigid framework. A theoretical study of oligo-fluorenes and fluorenones found that eximer precursors were unlikely to form cofacial pairs in both the parallel **1** and antiparallel **2** arrangements, and that study did not include any steric hindrance of a rigid framework to maintain interligand distances.[49] Chen et al. described two unique Zn(II)−norfloxin networks where the more π-stacked arrangement showed nearly double the QY of the tilted structure.[27] This is in contrast to the findings of the work of Bauer et al. on zinc−stilbene frameworks where cofacial dimers were shown to be detrimental to quantum yield; however, those structures were more flexible and the differences in the interactions of the ligand with itself and the extended structure prevent direct comparison.[34]

Thermal Stability. The first dehydration step of **1** is at 108 °C, and the first dehydration step of **2** begins around 70 °C. Detailed thermal gravimetric analysis in air and N_2 of **1** and **2** are given in the Supporting Information.

Conclusions

A new approach to the development of solid state lighting phosphors has been presented. Luminescent molecules like fluorenone and its derivatives have long been used in strictly organic applications where it has been cross-linked into polymers[50] and combined into OLEDs.[51] Similarly, the inorganic−organic framework structure has been used with both metal centered and antenna type structures with potential applications in sensors and scintillators. This is the first report, to our knowledge, of inorganic−organic frameworks based upon this ligand. It is also the first example of a ligand-centered luminescent framework that, in terms of excitation and emission spectra, meets most of the requirements for solid state lighting. The photoluminescence of both **1** and **2** can be excited in the near UV and blue, between 380 and 460 nm, and give broad emissions that peak at 503 and 526 nm, respectively. With FWHMs of around 90 nm, the emission broadness is comparable to those of Ce^{3+}:YAG phosphors. In addition, the tunability required for high performance phosphor materials is provided by altering the structure. We do not yet have enough unique structures to directly correlate the color and quantum yield shifts with one or more of the proposed mechanisms. Color shifts could arise from solvent-like effects of the network and interligand interactions. Nonradiative losses in these compounds arise from thermal quenching, concentration quenching, spectral overlap, conformationally dependent interligand interactions, and possible impurities below the levels of our detection methods. Further investigations are being carried out to more fully reveal which of these mechanisms are present in these systems, a better understanding of which will help guide further development of high quantum yield phosphors.

The QY of **1** is three times that of the H_2FDC itself, demonstrating that the optical properties of an organic ligand can be enhanced within a hybrid framework structure. On the other hand, the fact that the QY of **2** is not very different from H_2FDC shows that such enhancement can be strongly dependent on the specifics of the structure. There are, however, a number of generic advantages of hybrid frameworks compared with inorganic phosphor materials. For example, they require much lower processing temperatures and do not depend on expensive, rare-earth elements for luminescence. Also, since they are solution processable, we expect that nanoparticles should be more readily synthesized and that they will not suffer from the structural imperfections that undermine the performance of inorganic nanoparticles.[52] However, **1** and **2** still fall well short in terms of the brightness and temperature dependent behavior requirements that are essential for commercial viability of a phosphor. Nevertheless, our findings point to the real possibility of finding high performance inorganic−organic phosphor systems, especially if the frameworks can be rendered more rigid than those described in the present work. Such systems would have potential for use in solid state lighting and other optical applications.

Acknowledgment. The authors thank Guang Wu for his advice on crystallography. J.F. and A.K.C. thank the Mitsubishi Chemical Center for Advanced Materials for their support and Naoto Kijima, Jeffery Gerbec, and Yasuo Shimomura for helpful discussion. Facilities at UCSB were supported by NSF DMR05-20415. A.W. was supported by the RISE program at the UCSB MRL. The Advanced Light Source is supported by the Director, Office of Science, Office of Basic Energy Sciences, of the U.S. Department of Energy under Contract No. DE-AC02-05CH11231. Use of the Advanced Photon Source was supported by the U.S. Department of Energy, Office of Science, Office of Basic Energy Sciences, under Contract No. DE-AC02-06CH11357. A.K.C. thanks the ERC for an Advanced Investigator Award.

Supporting Information Available: Crystallographic data files, thermal gravimetric analysis, and powder diffraction data. This material is available free of charge via the Internet at http://pubs.acs.org.

(49) Marcon, V.; van der Vegt, N.; Wegnet, G.; Raos, G. *J. Phys. Chem. B* **2006**, *110*, 5253–5261.
(50) Hayashi, S.; Inagi, S.; Fuchigami, T. *Macromolecules* **2009**, *42*, 3755.
(51) Abbel, R.; Grenier, C.; Pouderoijen, M. J.; Stouwdam, J. W.; Leclére, P. E. L. G.; Sijbesma, R. P.; Meijer, E. W.; Schenning, A. P. H. J. *J. Am. Chem. Soc.* **2009**, *131*, 833.
(52) Furman, J. D.; Gundiah, G.; Page, K.; Pizarro, N.; Cheetham, A. K. *Chem. Phys. Lett.* **2008**, *465*, 67–72.